

MIT Open Access Articles

Single-Ion Li⁺, Na⁺, and Mg²⁺ Solid Electrolytes Supported by a Mesoporous Anionic Cu–Azolate Metal–Organic Framework

The MIT Faculty has made this article openly available. **Please share** how this access benefits you. Your story matters.

Citation: Park, Sarah S., et al. "Single-Ion Li⁺, Na⁺, and Mg²⁺ Solid Electrolytes Supported by a Mesoporous Anionic Cu–Azolate Metal–Organic Framework." *Journal of the American Chemical Society*, vol. 139, no. 38, Sept. 2017, pp. 13260–63.

As Published: <http://dx.doi.org/10.1021/jacs.7b06197>

Publisher: American Chemical Society

Persistent URL: <http://hdl.handle.net/1721.1/117532>

Version: Author's final manuscript: final author's manuscript post peer review, without publisher's formatting or copy editing

Terms of Use: Article is made available in accordance with the publisher's policy and may be subject to US copyright law. Please refer to the publisher's site for terms of use.



Single-Ion Li⁺, Na⁺, and Mg²⁺ Solid Electrolytes Supported by a Mesoporous Anionic Cu-azolate MOF

Sarah S. Park,[†] Yuri Tulchinsky,[†] Mircea Dincă*

Department of Chemistry, Massachusetts Institute of Technology, 77 Massachusetts Avenue, Cambridge, MA 02139, United States

Supporting Information Placeholder

ABSTRACT: A novel Cu(II)-azolate metal-organic framework (MOF) with tubular pores undergoes a reversible single crystal to single crystal transition between neutral and anionic phases upon reaction with stoichiometric amounts of halide or pseudohalide salts. The stoichiometric transformation between the two phases allows loading of record amounts of charge-balancing Li⁺, Na⁺, and Mg²⁺ ions for MOFs. Whereas the halide/pseudohalide anions are bound to the metal centers and thus stationary, the cations move freely within the one-dimensional pores, giving rise to single-ion solid electrolytes. The respective Li⁺, Na⁺, and Mg²⁺-loaded materials exhibit high ionic conductivity values of 4.4×10^{-5} S/cm, 1.8×10^{-5} S/cm, 8.8×10^{-7} S/cm. With addition of LiBF₄, the Li⁺ conductivity improves to 4.8×10^{-4} S/cm. These are the highest values yet observed for MOF solid electrolytes.

Safety concerns, lack of mechanical robustness, and processing difficulties drive current research on novel solid electrolytes.^{1,2} An attractive approach to developing such electrolytes is the concept of “single-ion” conduction.³ In liquid electrolytes, both anions and cations are mobile, although only the latter require mobility for a functioning battery. The anions need not be mobile, yet their mobility leads to polarization effects, which decrease the operating voltage of the cell. Accumulation of anions at the anode also eventually leads to decomposition of the liquid electrolyte, one of the primary culprits for declining battery performance over time. In single-ion solid conductors, the anions are fixed to the underlying matrix. This prevents anion movement and accumulation and eliminates the polarization effects present in liquid electrolytes.^{3,4} Although most recent research on single ion conductors has been in the context of Li-ion batteries, Na- and Mg-ion batteries are expected to benefit from the development of single-ion Na⁺ and Mg²⁺ conductors as well. Here, we show that a new Cu-azolate MOF that allows stoichiometric binding of anions functions as a good conductor for Li⁺, Na⁺, and Mg²⁺ ions. The respective ionic conductivities are the highest for this class materials in the absence of additional anion mobility.

MOFs are excellent platforms for exploring single-ion conductors. They are electrical insulators, are compatible with a wide range of mobile cations, are tunable, and present regular pore networks that allow, in principle, for swift ion movement. The potential impact of these materials as solid electrolytes has been confirmed by numerous examples of high proton conductivity,⁵ but reports of Li⁺, Na⁺, or Mg²⁺ ion conductors are decidedly more rare.⁶⁻⁹

Despite difficulties, several strategies have proven successful in introducing free Li⁺, Na⁺, or Mg²⁺ ions in MOFs. For instance, open metal sites in MOFs may be used to immobilize anions, leaving free, charge-balancing cations in the pores.⁷ Although successful in the preparation of the first Li⁺ and Mg²⁺ MOF-based solid electrolytes from Mg₂(2,5-dihydroxyterephthalate) (Mg-MOF-74), there is limited driving force for binding anions to metal sites in neutral compounds. The maximal Li⁺ and Mg²⁺ loading using this strategy was 1.26 wt% and 2.51 wt%, respectively, not counting cation content pertaining to free electrolyte. An alternative strategy is the post-synthetic functionalization of inorganic secondary building units (SBUs), such as dehydrating and grafting of LiO^tBu in Zr₆O₄(OH)₄(terephthalate)₆ (UiO-66).⁸ A third approach is the aliovalent substitution of trivalent ions in a MOF SBU by a combination of divalent and monovalent ions, the former replacing the trivalent ion structurally, with the latter remaining mobile.⁹ Neither of the last two strategies are quantitative, however. Indeed, grafting and substitution are both substoichiometric, and have led to maximal mobile Li⁺ loadings of 1.06 wt% and 0.08 wt%, respectively, and mobile Na⁺ loadings of 0.26 wt%. Our strategy herein allows for Li⁺, Na⁺, and Mg²⁺ loadings that exceed previous reports, providing a potential blueprint for optimizing ion carrier density in MOF solid electrolytes.

Solvothermal reaction between bis(1H-1,2,3-triazolo[4,5-*b*],[4',5'-*i*])dibenzo-[1,4]dioxin (H₂BTDD) and CuCl₂·2H₂O in an acidic mixture of *N,N*-dimethylformamide (DMF) and isopropyl alcohol at 65 °C yields emerald-green crystals of ((CH₃)₂NH₂)[Cu₂Cl₃BTDD]:(DMF)₄(H₂O)_{4,5} (**MIT-20**). X-ray diffraction analysis of **MIT-20** revealed a structure consisting of infinite linearly-bridged Cu SBUs with a single crystallographically unique Cu atom. Each Cu²⁺ ion displays a square pyramidal geometry and is coordinated by three independent triazolate ligands, disposed equatorially, and two chlorides, one terminal equatorial, the other bridging to a neighboring Cu atom (Figure 1). Alternate pairs of Cu atoms are connected either by two BTDD²⁻ ligands, or by two BTDD²⁻ ligands and a μ₂-Cl. The infinite Cu SBUs are connected by BTDD²⁻ linkers and line one-dimensional hexagonal channels with a crystallographic diameter of ~22 Å. The structure of **MIT-20** is similar to BTDD-based MOFs reported with Mn, Co, and Ni,¹⁰ and is topologically identical to the MOF-74 series, but differs from these in one critical aspect: whereas the latter are neutral, **MIT-20** is *formally anionic*, with the charge balance provided by free dimethylammonium (DMA) cations.

The free DMA suggested that **MIT-20** could function as a host for various cationic species, including Li⁺, Na⁺, or Mg²⁺, and thus provide a platform for developing solid electrolytes in the pres-

ence of appropriate solvents. To test this hypothesis, we subjected **MIT-20** to a Soxhlet extraction with hot methanol to remove residual DMF. During this treatment, the initially emerald green crystals gradually turned greenish-yellow (Figure S2), but retained their single-crystal nature. To our surprise, X-ray analysis of one of these resulting crystals revealed that methanol treatment removes one full equivalent of DMACl from **MIT-20** to provide *an overall neutral framework* where all remaining halides are bridging (Figure 1). Cu atoms in this neutral phase are octahedral, with a methanol molecule completing the coordination sphere along with three *mer*-oriented triazolates and two *trans*-oriented μ_2 -chlorides (Figure S3). Heating a single crystal of the greenish-yellow neutral phase to 100 °C led to a color change to dark red (Figure S2). Single crystal X-ray diffraction analysis revealed that this colour change is associated with the loss of the methanol molecule and formation of $\text{Cu}_2\text{Cl}_2\text{BTDD}$ (**MIT-20d**). **MIT-20d** exhibits square pyramidal Cu centers with *mer*-oriented triazolate linkers and *trans*- μ_2 -chlorides and is identical to those of $\text{M}_2\text{Cl}_2\text{BTDD}$ (M = Mn, Co, Ni) (Figure 1).¹⁰

N_2 adsorption analysis for **MIT-20d** at 77 K revealed a type IV isotherm, indicative of mesoporosity, with a total uptake of $\sim 750 \text{ cm}^3/\text{g}$ (Figure S5). Fits to this isotherm gave a Brunauer-Emmett-Teller (BET) apparent surface area of $2066 \text{ m}^2/\text{g}$ and a pore size distribution peaking at 22.5 \AA (Figure S6), in line with the value expected from crystallography (ca. 23 \AA) and with the values reported for other $\text{M}_2\text{Cl}_2\text{BTDD}$ materials.¹⁰

The preferential formation of anionic **MIT-20** under solvothermal conditions suggests that Cu^{2+} is unique among late first row transition metals in thermodynamically favoring the anionic phase over the neutral one under high chloride concentration. As such, we surmised that treatment of neutral **MIT-20d** with metal halides would quantitatively yield anionic phases with a large content of free metal cations residing in the pores. Indeed, treatment of **MIT-20d** with one equivalent of LiCl in dry tetrahydrofuran (THF) afforded a green microcrystalline powder exhibiting a PXRD pattern identical to that of **MIT-20** (Fig. S7). Exchange of residual THF with propylene carbonate (PC), a less volatile solvent with a higher dielectric constant that promotes Li ion conductivity yielded $\text{Li}[\text{Cu}_2\text{Cl}_3\text{BTDD}] \cdot 10(\text{PC})$ (**MIT-20-LiCl**) as a free-flowing powder. Inductively-coupled plasma mass spectrometry (ICP-MS) analysis of **MIT-20-LiCl** confirmed a Li:Cu ratio of 1:2. This ratio did not increase even when **MIT-20d** was treated with excess LiCl, suggesting that the Li content in **MIT-20-LiCl**, 1.38 wt%, is maximized. Importantly, ICP-MS confirmed that extensive washing and soaking for 7 days with dry THF at room temperature did not reduce the Li content of **MIT-20-Li**, thus attesting the strong binding of Cl^- to Cu^{2+} ions in this material.

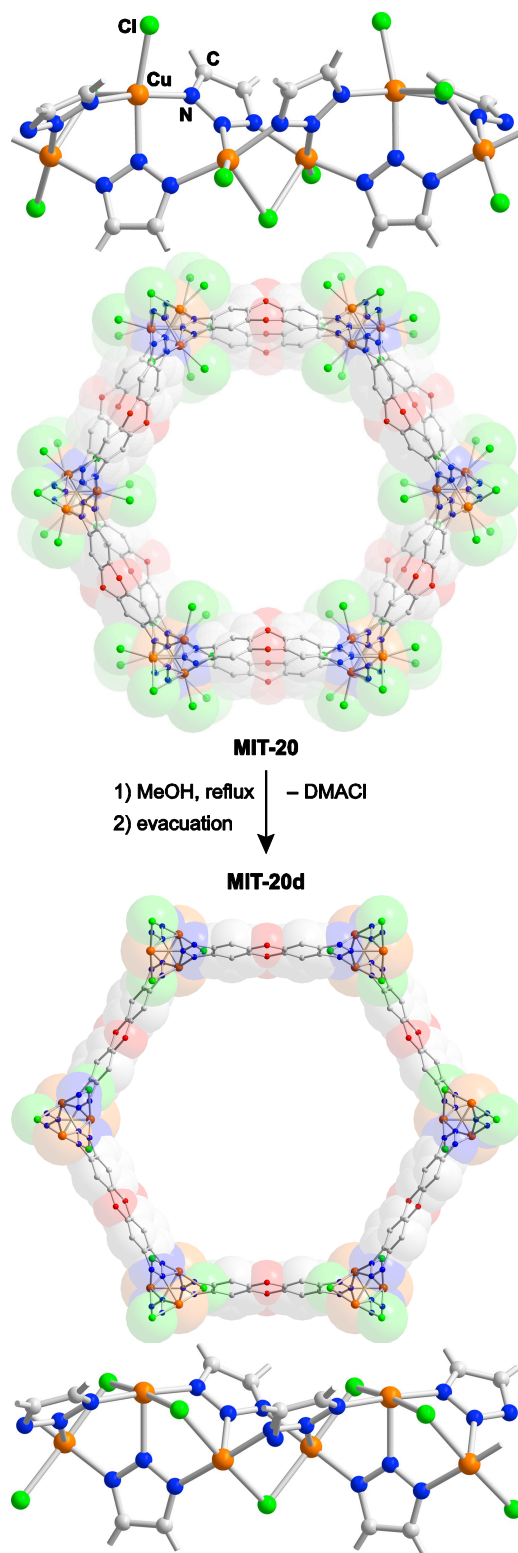


Figure 1. X-ray crystal structures of **MIT-20** and **MIT-20d**, formed from the former by loss of DMACl. The structures of **MIT-20-X** (X = LiCl, LiBr, Na, Mg), are analogous to **MIT-20**. H atoms are omitted for clarity.

The isolation of free cations in the pores of **MIT-20** by reacting neutral **MIT-20d** with metal halides is not limited to Li^+ . Although NaCl and MgCl_2 are nearly insoluble in THF, we were able to access Na^+ and Mg^{2+} -substituted analogs of **MIT-20** by react-

ing **MIT-20d** with one equivalent of NaSCN or MgBr₂. Upon exchange of residual THF with PC, this led to quantitative formation of Na[Cu₂Cl₂(SCN)BTDD]·9(PC) (**MIT-20-Na**) and Mg_{0.5}[Cu₂Cl₂BrBTDD]·8(PC) (**MIT-20-Mg**), respectively, which exhibit record contents of mobile Na⁺ and Mg²⁺ ions of 4.23 wt% and 3.76 wt%, respectively. In all cases, structural retention was verified by PXRD analysis (Figure S7) and the precise content of PC, quantified by ¹H NMR of solutions obtained by digesting the respective MOFs (Figure S8), were in line with those observed by TGA (Figure S9). Infrared spectroscopy of **MIT-20-Na** showed a C–N stretching mode at 2099 cm⁻¹, indicative of metal-bound SCN⁻, and no residual peaks for free SCN⁻ (ν_{CN} = 2074 cm⁻¹) (Figure S10).¹¹ This provided additional evidence that all SCN⁻ anions in **MIT-20-Na** are immobile.

Ionic conductivity measurements for **MIT-20-X** (X = LiCl, Na, Mg) were performed on powder pellets using alternating current (ac) impedance spectroscopy. Pellets were sandwiched between two stainless steel electrodes under dry N₂ in an air-tight cell. Under these conditions, the Nyquist plots obtained for **MIT-20-X**, shown in Figure 2, exhibit a semi-circle at high frequency and a linear tail at low frequency. The latter is commonly attributed to blocking effects at the electrode and is typical for ionic conductors.⁷⁻⁹ These plots revealed similar Li⁺ and Na⁺ conductivity values of 1.3 × 10⁻⁵ S/cm and 1.8 × 10⁻⁵ S/cm for **MIT-20-LiCl** and **MIT-20-Na**, respectively, at 25 °C (Table 1). The value for Li⁺ is of the same magnitude as those of Mg₂(dobdc)·0.06LiO¹Pr (σ = 1.2 × 10⁻⁵ S/cm)^{7a} and LiO¹Bu-grafted UiO-66 (σ = 1.8 × 10⁻⁵ S/cm),⁸ whereas the conductivity of Na⁺ is considerably higher than that of Mn@EHU1(Sc,Na) (σ = 2.0 × 10⁻⁶ S/cm).⁹ The Mg²⁺ ion conductivity in **MIT-20-Mg** was lower, 8.8 × 10⁻⁷ S/cm, as expected for the transport of divalent ions carrying a higher charge density through the otherwise conserved electric field environment of **MIT-20**. To exclude the contribution of electronic conduction, we measured current-voltage curves for Cu₂Cl₂BTDD(DMF)₂ (Figure S11), which confirmed an electrically insulating behavior, with a conductivity of only 10⁻¹⁴ S/cm in N₂ atmosphere at 25 °C (Figure S12).

To determine the portion of current carried by lithium ions in **MIT-20-LiCl**, we conducted lithium transference number measurements using a potentiostatic polarization method.¹² The transference number was t_{Li+} = 0.66 (±0.031), with certain devices reaching numbers as high as t_{Li+} = 0.75 (Figure S13). These are significantly higher than the values observed for liquid lithium-ion electrolytes, typically less than 0.4,¹³ and support our assertion that the current carried by **MIT-20-LiCl** is dominated by Li⁺ transport.

One approach to changing the polarity of the pore and potentially increasing the conductivity is the installation of softer, less electronegative anions that interact more weakly with the mobile cations, thereby decreasing the activation energy for transport.⁸ Owing to its unique ability to allow for large cation loading, **MIT-20** is well suited for this purpose. Indeed, reaction of **MIT-20** with LiBr followed by exchange of solvent led to the isolation of Li_{0.8}[Cu₂Cl₂Br_{0.8}BTDD]·10(PC) (**MIT-20-LiBr**). Remarkably, even though the molar Li⁺ content of this material is 20% lower than that of **MIT-20-LiCl**, its conductivity was higher, 4.4 × 10⁻⁵ S/cm, as determined by ac impedance spectroscopy. Furthermore, soaking **MIT-20-LiBr** in a 1 M solution of LiBF₄ in PC yielded Li_{0.9}[Cu₂Cl₂Br_{0.9}BTDD]·0.3LiBF₄·9(PC) (**MIT-20-LiBF₄**) with a Li-ion conductivity of 4.8 × 10⁻⁴ S/cm. This value is comparable, and indeed exceeds the Li conductivity values observed for other MOF-based Li-ion conductors, including Mg₂(dobdc)·0.35LiO¹Pr·0.25LiBF₄ (σ_{Li} = 2.4 × 10⁻⁴ S/cm)^{7a} and EHU1(Sc,Li)·(LiBF₄) (σ_{Li} = 4.2 × 10⁻⁴ S/cm).⁹

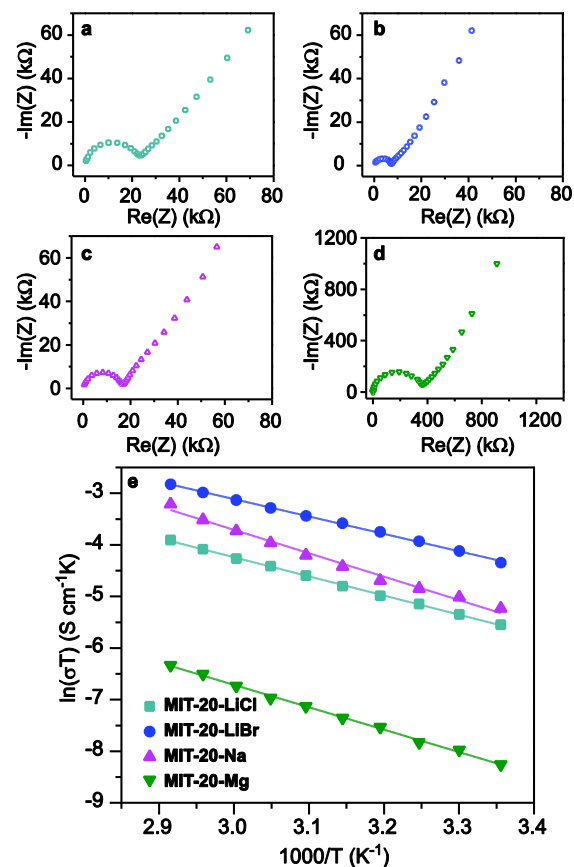


Figure 2. Nyquist plots for (a) **MIT-20-LiCl** (b) **MIT-20-LiBr**, (c) **MIT-20-Na**, and (d) **MIT-20-Mg**. (e) Ionic conductivities as a function of temperature in the range of 25 °C to 70 °C.

To ascertain the influence of the pore environment and cation identity on conductivity, we determined the activation energy for ion transport by collecting variable-temperature ac impedance data between 25 °C and 70 °C (Figure S15). PXRD analysis after these measurements indicated no significant loss in crystallinity (Figure S16), while infrared spectroscopy showed that all SCN⁻ remained bound within **MIT-20-Na** (Figure S10). Thus, our materials maintain structural integrity during ion transport measurements. As shown in Figure 2 and Table 1, the activation energy for Li transport in **MIT-20-LiBr**, 0.29 eV, is indeed lower than that for **MIT-20-LiCl**, 0.32 eV, which suggests that further systematic changes in anion identity may improve the ionic conductivity in **MIT-20-X**, as also shown previously with MOF-74-type materials.^{7b} The very low activation energy found for **MIT-20-LiBF₄**, 0.16 eV (Figure S18, highlights that our new solid electrolyte, synthesized by an unprecedented phase change in a MOF, can be classified as a superionic conductor, defined as a material with a conductivity of 10⁻⁴ S/cm and an activation energy smaller than 0.4 eV.¹⁴

Table 1. Ionic conductivity and activation energies for **MIT-20-X** (X = LiCl, LiBr, LiBF₄, Na, Mg).

compound	Mobile ion	Guest per mole MOF	σ (S/cm)	E _a (eV)	PC per mole of MOF
MIT-20-LiCl	Li ⁺	1	1.3 × 10 ⁻⁵	0.32	10.3
MIT-20-LiBr	Li ⁺	0.8	4.4 × 10 ⁻⁵	0.29	10.3

MIT-20-LiBF₄	Li ⁺	1.2	4.8 × 10 ⁻⁴	0.16	8.7
MIT-20-Na	Na ⁺	1	1.8 × 10 ⁻⁵	0.39	9.3
MIT-20-Mg	Mg ²⁺	0.5	8.8 × 10 ⁻⁷	0.37	8.2

In summary, the reversible phase transitions from an anionic phase to a neutral one supported by a new copper azolate MOF enable the isolation of stoichiometric amounts of mobile Li⁺, Na⁺, and Mg²⁺ ions in one-dimensional mesopores. The respective Li⁺-, Na⁺-, and Mg²⁺-loaded materials function as single-ion solid electrolytes, with conductivity values that are among the highest or exceed other materials in this class, and activation energies that depend on the nature of the immobile anions. The strategy reported here is enabled by the thermodynamic stability of the anionic MOF phase, its formation presenting a strong driving force for the immobilization of large molar amounts of free ions. Additional, non-stoichiometric Li⁺ ions further improve the ionic conductivity above 10⁻⁴ S/cm, placing an MIT-20-derived electrolyte as superionic conductor. Identification of other anionic MOFs that become neutral upon loss of stoichiometric salt equivalents may serve as a blueprint for the design of other single-ion electrolytes.

ASSOCIATED CONTENT

Supporting Information

Synthetic details, single crystal and powder X-ray diffraction data, N₂ adsorption isotherms, TGA, NMR and ac impedance spectra. This material is available free of charge via the Internet at <http://pubs.acs.org>.

AUTHOR INFORMATION

Corresponding Author

*mdinca@mit.edu

Author Contributions

† S.S.P. and Y. T. contributed equally.

Notes

The authors declare no competing financial interests.

ACKNOWLEDGMENT

This work was supported by the National Science Foundation, through the Waterman Award to M.D. (DMR-1645232). S.S.P. is partially supported by a NSF GRFP (Award No. 1122374). M.D. gratefully acknowledges early career support from the Sloan Foundation, the Research Corporation for Science Advancement, and the Dreyfus Foundation. We thank Dr. P. Mueller and Dr. J. Becker for assistance with crystallography, Prof. J. F. Van Humbeck for assistance with the ac impedance experimental setup, Dr.

S. Zhang for helpful discussions on dc measurements, and Dr. L. Sun for electrical conductivity measurements.

REFERENCES

- (a) Tarascon, J.-M.; Armand, M. *Nature* **2001**, *414*, 359. (b) Xu, K. *Chem. Rev.* **2004**, *104*, 4303. (c) Goodenough, J. B.; Kim, Y. *Chem. Mater.* **2010**, *22*, 587.
- (a) Meyer, W. H. *Adv. Mater.* **1998**, *10*, 439. (b) Croce, F.; Appetecchi, G. B.; Persi, L.; Scrosati, B. *Nature* **1998**, *394*, 456. (c) Fergus, J. W. *J. Power Sources* **2010**, *195*, 4554. (d) Kamaya, N.; Homma, K.; Yamakawa, Y.; Hirayama, M.; Kanno, R.; Yonemura, M.; Kamiyama, T.; Kato, Y.; Hama, S.; Kawamoto, K.; Mitsui, A. *Nat. Mater.* **2011**, *10*, 682.
- (a) Wright, P. V. *MRS Bull.* **2002**, *27*, 597. (b) Van Humbeck, J. F.; Aubrey, M. L.; Alsaiee, A.; Ameloot, R.; Coates, G. W.; Dichtel, W. R.; Long, J. R. *Chem. Sci.* **2015**, *6*, 5499.
- (a) Doyle, M.; Fuller, T. F.; Newman, J. *Electrochim. Acta* **1994**, *39*, 2073. (b) Sadoway, D. R.; Huang, B.; Trapa, P. E.; Soo, P. P.; Bannerjee, P.; Mayes, A. M. *J. Power Sources* **2001**, *97*, 621. (c) Lin, K.-J.; Li, K.; Maranas, J. K. *RSC Adv.* **2013**, *3*, 1564. (d) Zugmann, S.; Gores, H. J. *Transference Numbers of Ions in Electrolytes*. In *Encyclopedia of Applied Electrochemistry*; Kreysa, G., Ota, K., Savinell, R. F., Eds.; Springer: New York, New York, NY, 2014; pp 2086-2091.
- (a) Horike, S.; Umeyama, D.; Kitagawa, S. *Acc. Chem. Res.* **2013**, *46*, 2376. (b) Yoon, M.; Suh, K.; Natarajan, S.; Kim, K. *Angew. Chem. Int. Ed.* **2013**, *52*, 2688. (c) Yamada, T.; Otsubo, K.; Makiura, R.; Kitagawa, H. *Chem. Soc. Rev.* **2013**, *42*, 6655. (d) Ramaswamy, P.; Wong, N. E.; Shimizu, G. K. H. *Chem. Soc. Rev.* **2014**, *43*, 5913.
- (a) Zhang, A.; Yoshikawa H.; Awaga, K. *J. Am. Chem. Soc.* **2014**, *136*, 16112. (b) Fujie, K.; Ikeda, R.; Otsubo, K.; Yamada, T.; Kitagawa, H. *Chem. Mater.* **2015**, *27*, 7355. (c) Aubrey, M. L.; Long, J. R. *J. Am. Chem. Soc.* **2015**, *137*, 13594. (d) Vazquez-Molina, D. A.; Mohammad-Pour, G. S.; Lee, C.; Logan, M. W.; Duan, X.; Harper, J. K.; Uribe-Romo, F. J. *J. Am. Chem. Soc.* **2016**, *138*, 9767. (e) Bai, L.; Tu, B.; Qi, Y.; Gao, Q.; Liu, D.; Liu, Z.; Zhao, L.; Li, Q.; Zhao, Y. *Chem. Commun.* **2016**, *52*, 3003.
- (a) Wiers, B. M.; Foo, M.-L.; Balsara, N. P.; Long, J. R. *J. Am. Chem. Soc.* **2011**, *133*, 14522. (b) Aubrey, M. L.; Ameloot, R.; Wiers, B. M.; Long, J. R. *Energy Environ. Sci.* **2014**, *7*, 667.
- Ameloot, R.; Aubrey, M.; Wiers, B. M.; Gómora-Figueroa, A. P.; Patel, S. N.; Balsara, N. P.; Long, J. R. *Chem. Eur. J.* **2013**, *19*, 5533.
- Cepeda, J.; Pérez-Yáñez, S.; Beobide, G.; Castillo, O.; Goikolea, E.; Aguesse, F.; Garrido, L.; Luque, A.; Wright, P. A. *Chem. Mater.* **2016**, *28*, 2519.
- (a) Rieth, A. J.; Tulchinsky, Y.; Dincă, M. *J. Am. Chem. Soc.* **2016**, *138*, 9401. (b) Rieth, A. J.; Yang, S.; Wang, E. N.; Dincă, M. *ACS Cent. Sci.* **2017**, *3*, 668.
- Tian, J.-L.; Xie, M.-J.; Liu, Z.-Q.; Yan, S.-P.; Liao, D.-Z.; Jiang, Z.-H. *J. Coord. Chem.* **2015**, *58*, 833.
- Evans, J.; Vincent, C. A.; Bruce, P. G. *Polymer* **1987**, *28*, 2324.
- (a) Dia, H.; Zawodzinski, T. A. *J. Electroanal. Chem.* **1998**, *459*, 111. (b) Mussini, P. R.; Mussini, T.; Sala, B. *Phys. Chem. Chem. Phys.* **1999**, *1*, 5685. (c) Zhao, J.; Wang, L.; He, X.; Wan, C.; Jiang, C. *J. Electrochem. Soc.* **2008**, *155*, A292. (d) Zugmann, S.; Fleischmann, M.; Amereller, M.; Gschwind, R. M.; Wiemhöfer, H. D.; Gores, H. J. *Electrochim. Acta* **2011**, *56*, 3926.
- Linford, R.G.; Hackwood, S. *Chem. Rev.* **1981**, *81*, 327.

TOC graphic

